Finite Element Modeling of Direct Shear Transfer in Carbon Fiber Reinforced Concrete

By Mohamed M. Safan

Lecturer (Dep. of Civil Eng., Faculty of Eng., Menoufia University, Egypt)

Abstract: *A finite element analysis is presented to simulate the behavior of push-off specimens under direct shear. The model incorporates the material parameters for reinforcement and the concrete matrix reinforced with carbon fibers. The experimental results available in the literature were used to validate the numerical results. Design equations according to the shear-friction concept reported by the ACI code were revised for sand-lightweight carbon fiber concrete. A more rational design equation was proposed for this type of concrete.*

Keywords: Direct shear; friction reinforcement; carbon fiber concrete; finite elements.

Introduction:

Shear failures in reinforced concrete members have an abrupt nature and due to the difficulty in formulating reliable mechanical analyses of shear behavior, research efforts concentrated on predicting the collapse load, usually on an empirical basis. Applications exist where direct shear transfer failures rather that diagonal tension failures are appropriate to consider as in case of an existing or a potential crack, an interface between concretes cast at different times, an interface between concrete and a dissimilar material and connections in precast constructions. The shear-friction concept provides a convenient tool for direct shear design. The approach is to assume that a crack has formed at an expected location. As slip begins to occur along the crack, the roughness of the crack surface forces the opposing faces of the crack to separate. This separation is resisted by the reinforcement across the crack. At ultimate, the separation is sufficient to stress the reinforcement to yield and thus, a clamping force $A_{fr} f_y$ is generated across the crack. The shearing force is thus resisted by friction along the crack faces, aggregate interlock, and possibly dowel action [1].

Manuscript received from Dr . Mohamed M.Safan
Accepted on : 3 / 9 / 2003
Engineering Research Journal Vol 26, No 4, 2003 Minufiya University, Faculty Of Engineering , Shebien El-Kom , Egypt , ISSN 1110-1180

The amount of load transferred by dowel action was found to depend on the amount and distribution of reinforcement and the relative movement of the crack surfaces [2]. On the other hand, the load percentage transferred by friction and aggregate interlock depends on crack width, bond effectiveness, and reinforcement anchorage [3,4,5].

Carbon fiber reinforced concrete is a structural materials that is gaining an importance due to the decrease in carbon fiber cost and the increasing demand of superior structural and functional properties. Research conducted so far with large steel fibers (20 to 60 mm in length and about 0.3 to 1.0 mm in diameter) indicated that while toughness improvements were significant, tensile strength of the composite was not greatly different from that of the host matrix [11]. Tensile failure is caused by the progressive extension of distributed micro-cracks that eventually coalesce into macro-cracks. Large steel fibers are too far apart to arrest or modify these micro-cracks. For an improvement in the tensile strength, extremely fine fibers (<25μm) are needed. Carbon fibers, satisfying this requirement, also offer many advantages over other fiber types (steel, polypropylene, glass, etc.) such as finishability, thermal resistance, weatherability, no rust stain problems, the possibility of accelerated curing at elevated temperatures without degrading the fibers [12] and long-term chemical stability in aggressive environments.

This research aims to investigate the possibility of simulating the behavior of push-off specimens cast with Carbon Fiber Reinforced Concrete (CFRC) by Finite element modeling to predict ultimate shear transfer capacity as well as the failure mechanism. For this purpose important parameters related to the generation of the FE mesh should be considered. For instant, the ultimate load computation is influenced by the type of the element, while computation of failure mechanisms in softening materials is affected by both the type of the element and how the elements are arranged to form the FE mesh. Also, finite elements tend to diffuse sharp gradients and discontinuities such as shear bands over elements. Sometimes, the result makes it difficult to identify the failure mechanism and gives a less fragile load-displacement response with an ultimate load that can be higher than the real, which means that the prediction gives over-conservative results. The results of the analytical experiments by Pastro et al. [6] indicated the convenience of using a mesh of simple triangles aligned following the direction of the shear band and having a width small enough to provide adequate resolution of the band. These important guidelines considering the element type, size, and alignment were successfully adopted in the current research.

Theoretical basis of shear-friction design

The shear-friction concept assumes that a shear crack can be formed in an unfavorable location despite the relatively high strength of concrete in direct shear and that reinforcement must be provided across the crack to resist relative displacement. The shear-friction design method according to the ACI building code [7] assumes that all the shear resistance is due to friction between the crack faces. When the reinforcement is normal to the shear plane, The nominal shear strength V_n is given by

$$V_n = \rho f_y \mu \qquad (1)$$

but not greater than $0.2 f'_c$ nor 5.6 MPa. Appropriate values for the coefficient of friction μ are used, depending on the nature of the interface, so that the estimated strength will be in good agreement with test results. For normal weight concrete, the coefficient of friction takes a value of 1.4 for monolithically cast concrete. This value is reduced by a factor of 0.85 for sand-lightweight concrete. The above equation results in a conservative prediction of the shear-transfer strength. Based on test results, Mattock [8,9] showed that when the reinforcement is normal to the shear plane, the shear strength could be better expressed as

$$V_n = 0.8\rho f_y + K \qquad (2)$$

the second term K represents the influence of the dowel action and aggregate interlock and takes values of 2.8 and 1.75 MPa for normal and sand-lightweight concrete, respectively. The shear strength should not be more than $0.3 f'_c$ for normal strength concrete and not more than $0.2 f'_c$ nor 7.0 MPa for sand-lightweight concrete. Specifying an upper limit on the shear-transfer strength effectively limits the amount of maximum reinforcement.

Shear transfer capacity of normal weight concrete was found to be consistently higher than that of lightweight concrete for the same amount of reinforcement and approximately the same compressive strength. This was attributed to the observation that bond strength between the mortar and aggregate particles is usually greater than the tensile strength of the aggregate particles [10]. Therefore, the cracks propagate through the aggregate particles instead of around them resulting in more relative movement about the interface and smaller shear transfer capacity.

Research Significance:

As the ACI building code does not address the shear properties of CFRC and design equations are needed to predict the shear transfer capacity of this type of concrete, a comprehensive analysis is needed because of the complicated nature of shear failures. A finite element analysis is presented in this research to investigate the

behavior of RC push-off specimens. The argument that the influence of different CF contents on the shear behavior can be simulated by applying the mechanical properties of the corresponding concrete mixes was examined. Three mechanical properties, the cylinder compressive strength, splitting tensile strength, and modulus of elasticity were applied attempting to introduce the influence of CF content on the shear behavior. The mechanical properties and test results reported in a recent research [13] for sand-lightweight CFRC specimens were used to verify the capability of the proposed analysis to predict the shear behavior in terms of ultimate loads, displacements, and failure mechanisms.

Concrete and reinforcing steel material models:

The SBETA constitutive model [14,15] was applied to simulate the behavior of concrete. The model is rather simple to use as only the cube compressive strength is needed to define the material parameters. Automatic generation of the values of these parameters is done according to the formulas provided by the CEB-FIP Model Code 90 [16] and other research sources [15]. However, typical values for the cylinder compressive strength f'_c, splitting tensile strength f_{ct}, and modulus of elasticity E were explicitly defined. The adopted values of these parameters for ordinary concrete and CFRC mixes are given in Table (1).

Table (1): Mechanical properties for cylinder samples with different carbon fiber contents (MPa)

C.F., %	f'_c	f_{ct}	E
0.00	47.0	3.37	290 73
0.50	35.1	3.30	227 53
1.00	22.8	2.77	179 07
1.25	13.3	2.04	131 32

The main features of the concrete material model included a non-linear behavior in compression with hardening and softening. Softening in compression is modeled by linearly descending branch based on dissipated energy. Modeling of concrete fracture in tension is based on the non-linear fracture mechanics. A fictitious crack model based on fracture energy and a crack opening low is used in combination with the crack band concept for convenient modeling of crack propagation in concrete. The shape of the crack-opening law and fracture energy are both defined as material properties. The use of fictitious tension plane model according to the crack band theory and an analogous one for modeling compression failure provide a convenient formulation to

eliminate the two deficiencies due to element size and element orientation effects. Cracked or crushed concrete is treated as an orthotropic material. The smeared crack model in which several parallel fissures are assumed to be evenly distributed throughout the material volume is adopted in the current analysis by introducing orthotropy in the material constitutive model. Along with this model, the fixed crack approach [14] is adopted assuming that the crack direction is given by the principle stress direction at the moment of crack initiation. During higher loading levels this direction is fixed and represents the material axis of orthotropy. Other features of the concrete material model included the use of reduction factors for the compressive strength and shear stiffness upon cracking. More details about the concrete material model can be found in [15].

The steel reinforcement was modeled as an elastic perfectly-plastic material and the reinforcing bars were modeled by truss elements as discrete bars with a uniaxial stress state. The concrete material model allowed for a rational simulation of the tension stiffening effect that refers to the contribution of cracked concrete to the tensile stiffness of reinforcing bars by proper modeling of discrete reinforcement and cracking in the surrounding concrete. An accurate analysis is thus possible by avoiding the overestimation of this effect associated with the traditional entry of an explicit tension stiffening factor in material models.

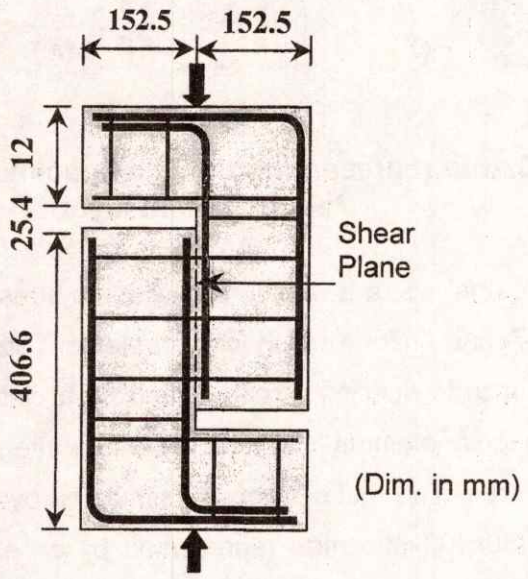

Fig. (1): Push-off RC specimen

Finite element modeling:

The FE model simulated the specimens tested by El-Mokadem [13]. The specimens were of the push-off type as shown in Fig. (1) with dimensions of 127x305x559 mm with two gaps to create the shear plane. When loaded as indicated, direct shear was produced on the shear plane (127x254 mm). The reinforcement crossing the shear plane was in the form of closed stirrups made of #3 bars (area = 70.88 mm^2 and f_y = 442 MPa) and thus, the reinforcement ratios for one, two, and three stirrups were 0.44, 0.88, and 1.32 percent of the shear plane area, respectively. The two cantilevers were reinforced with #5 bars with an L shape to insure integrity of the specimen to resist flexural failure in the cantilevers.

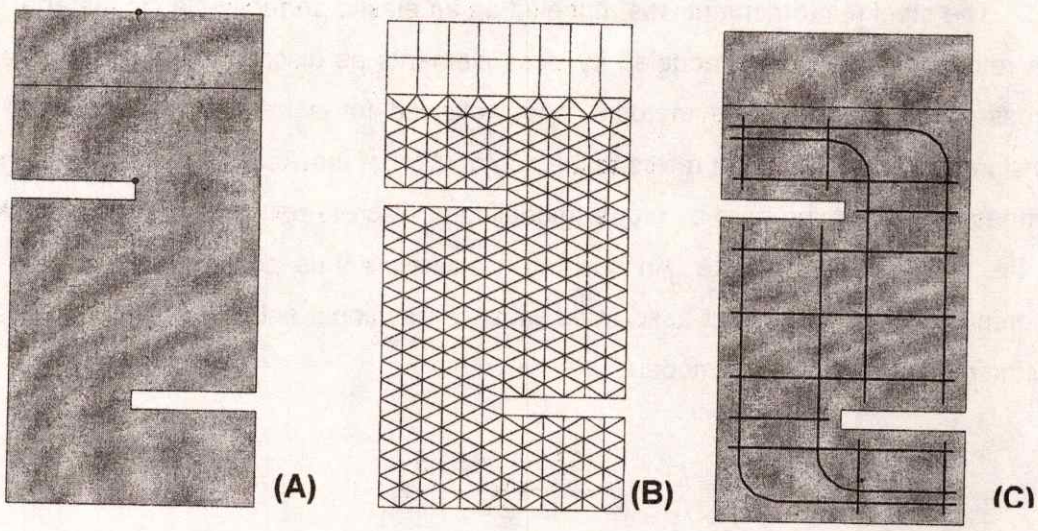

Fig. (2): (A) 2D area representing the test specimen, (B) FE mesh, and (C) reinforcement layout.

For the FE analysis, a two-dimensional plane stress idealization of the problem was considered. A fine uniform mesh with an element size of 25 mm was prescribed throughout the concrete specimen represented by a closed area. A simple 3-noded isoparametric triangular element integrated by Gauss integration at one point was used for meshing this area. The test set-up was simulated by applying the load through a rigid steel plate (50x100x305 mm) represented by an elastic isotropic material and meshed using 4-noded quadrilateral elements. The generated mesh is shown in Fig. (2.b). After the mesh was generated, the reinforcement bars were described and superposed over it. The discrete bars are then meshed by locating the intersections with the elements of the concrete body. This flexible representation allows for a free layout of the reinforcement independent of the underlying mesh. Vertical and horizontal displacements were restricted at the base of the specimen, while the load was applied

by prescribing vertical displacement at the middle point on top of the loading plate. Thus, the applied load would always be vertical while the top face of the test specimen rotated freely. To determine the maximum load-carrying capacity of the modeled specimens the FE solution should be capable of tracing the structural response in the post-peak regime. The Newton-Raphson solution method is sufficient for this purpose as displacement control is used for loading. To speed up convergence of the solution, the full Newton-Raphson method in which the tangent stiffness is updated in each iteration was adopted. The advanced line search technique was also used to automatically adjust the speed of the analysis according to the non-linearity of the response.

Analysis and discussions:

The experimental results summarized in Table (1) shows a continuous reduction in the compressive strength as the CF content increased. This reduction was due to an increase in the w/c ratio to maintain a specified degree of workability. However, the tensile strength considerably increased, as a percentage of the corresponding compressive strength, as the CF content increased. The shear behavior of 12 push-off specimens was analyzed. The analytical results were obtained for specimens with 1, 2 and three stirrups crossing the shear plane and CF contents of 0.0, 0.5, 1.0 and 1.25 percent of the total volume of the mix.

The analytical values for ultimate shear transfer strength, V_n, are shown in Table (2) along with the corresponding experimental values [13]. The ultimate shear strength is computed as a nominal stress by dividing the maximum shear load over the shear plane area. It can be seen that the shear capacity increased with the increase of the shear reinforcement ratio and decreased as the CF content increased as a result of the significant decrease in concrete compressive strength.

Slip and separation were experimentally measured [13] by monitoring the relative displacements at two points located at the middle of the specimen height and each 25 mm apart from the shear plane. The analytical values of slip and separation at peak loads along with the corresponding experimental values are given in Tables (3). The analytical values were averaged with an accuracy of 0.05 mm providing a reasonable estimate of both slip and separation. For a given FC content, slip and separation at peak load increased with the increase in the shear reinforcement crossing the shear plane. As the load increased, the reinforcement stretched allowing the formation of more cracks before the peak load is reached. For the same reinforcement ratio, the value of slip and separation at the peak load increased with the increase of CF content.

The presence of CF provided a similar behavior as shear reinforcement by bridging over the cracks, allowing the shear load to distribute over a larger area of concrete and increasing aggregate interlock capacity. The value of separation was higher than the associated slip in all specimens.

Table (2): Average maximum shear resisted by push-off specimens (MPa)

C.F., %	*Reinforcement Ratio (ρ), %*		
	0.44	0.88	1.32
0.00	9.34 (10.67)	10.18 (10.96)	10.94 (11.17)
0.50	8.16 (7.51)	8.74 (9.83)	9.38 (9.97)
1.00	6.87 (5.13)	6.91 (6.60)	7.44 (6.25)
1.25	4.71 (3.62)	4.87 (5.16)	5.7 (6.11)

( ) Experimental results [13]

Table (3): slip & separation at maximum load (mm)

C.F., %	*Reinforcement Ratio (ρ), %*		
	0.44	0.88	1.32
0.00 (slip)	0.05 (0.058)	0.15 (0.132)	0.15 (0.140)
(separation)	0.20 (0.193)	0.20 (0.218)	0.30 (0.254)
0.50	0.25 (0.287)	0.30 (0.292)	0.30 (0.300)
	0.40 (0.353)	0.40 (0.386)	0.40 (0.427)
1.00	0.30 (0.333)	0.40 (0.368)	0.40 (0.396)
	0.40 (0.376)	0.50 (0.445)	0.50 (0.488)
1.25	0.40 (0.384)	0.45 (0.400)	0.50 (0.414)
	0.40 (0.389)	0.45 (0.422)	0.55 (0.498)

( ) Experimental results [13]

The general behavior of the 12 specimens was similar in that no significant slip or separation occurred until the formation of tension cracks in the shear plane region. Cracking loads, corresponding to a cracking width of 0.05 mm, were in the range 60 to 70 percent of the corresponding ultimate loads. The initial cracks were inclined at 10 to 25^0 to the shear plane. As the load increased, more cracks developed and the inclination angle increased from 25 to 45^0 as the load approached peak load as can be seen in Fig. (3). Generally, the number of cracks at peak load increased as the number of stirrups crossing the shear plane increased. Also, more cracks developed at

peak loads as the CF content increased, while the cracking width was found to decrease as the CF content increased. Fig. (3) also demonstrates the distribution of tensile stresses in the reinforcement at three stages, before cracking, at cracking and at peak load for a specimen with one stirrup crossing the shear plane. The distribution clearly demonstrates the tension stiffening effect. When a crack opens to such an extent that concrete has no stiffness, the reinforcement takes up the tension previously carried by concrete which causes a localized increase in the tensile stress at the crack location.

Table (4): Maximum tensile stress in the reinforcement / yield load

C.F., %	*Reinforcement ratio (ρ)*		
	0.44	0.88	1.32
0.00	U / 1.00 / L *	0.73 / M / 0.80	0.50 / 0.70 / 0.53
0.50	U / 1.00 / L	0.65 / M / 0.72	0.46 / 0.63 / 0.50
1.00	U / 1.00 / L	0.57 / M / 0.64	0.39 / 0.53 / 0.46
1.25	U / 0.87 / L	0.52 / M / 0.49	0.31 / 0.38 / 0.30

* U: Upper rebar M: Middle rebar L: Lower rebar

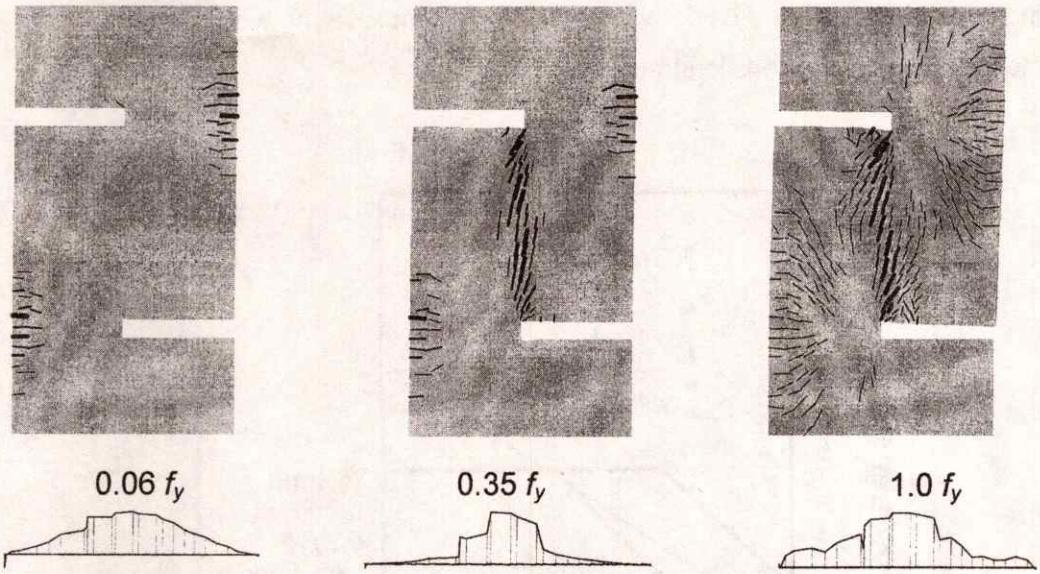

Fig. (3): Cracking pattern at different loading stages

Table (4) shows the numerical values for the maximum tensile stress developed in the reinforcement across the shear plane as a fraction of the yield stress. It can be noticed that the stress developed in the shear reinforcement was quite below the yield

point in nine specimens. The stress level decreased with the increase in the reinforcement ratio and reduction in the compressive strength as the CF content increased. Moreover, the more consistent numerical results in Table (2) shows only a marginal increase in the shear strength capacity as the reinforcement ratio increased, obviously due to low tensile stress levels in the shear reinforcement. This argument shows that the statement that the separation at the ultimate load is sufficient to stress the reinforcement to yield was not always satisfied within the scope of the available results. Numerical experiments were conducted to examine the satisfaction of this requirement applying Equation (2). Adopting an upper limit of 5.6 MPa (800 Psi) for the shear strength, Equation (2) yielded reinforcement ratios higher than required. The numerical results showed that the yield criterion is met for sand-lightweight CFRC by modifying Equation (2) to

$$V_n = 1.1\rho f_y + 2.8 \qquad (3)$$

but not greater than $0.2\, f'_c$ nor 5.6 MPa. The increase in the coefficient of friction (0.8 increased to 1.1) and the parameter K (1.75 increased to 2.8) is rational due to the action of carbon fibers leading to an improved shear behavior. Fig. (4) is a plot of Equations (1, 2 and 3) versus the discrete numerical and experimental result showing the adequacy of the proposed equation. It worth noting that the proposed formula should also be valid for CFRC mixes of higher compressive strength achieved by keeping w/c ratios fixed and using water reducers to improve the workability due to the expected increase in the tensile stress level.

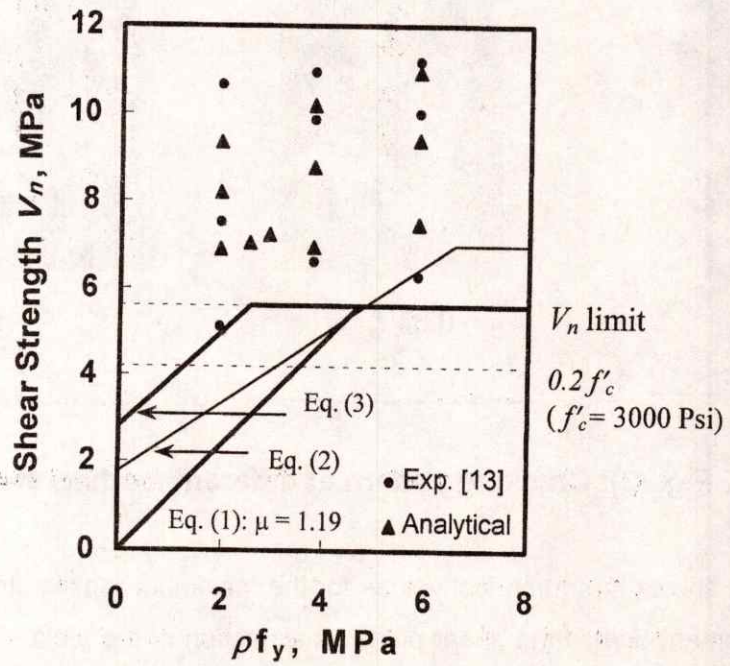

Fig.(4): Shear-friction design equations

Conclusions:

This paper presents a FE analysis for predicting the direct shear transfer capacity provided by sand-lightweight CFRC. The analytical results were verified by experimental results provided by push-off specimens. The analytical model predicted the direct shear behavior of these specimens quite well in terms of ultimate capacity, displacements and failure mechanism. It was verified that the influence of different CF contents on the direct shear behavior can be simulated by applying the mechanical properties of the corresponding concrete mix in terms of the cylinder compressive strength, splitting tensile strength, and modulus of elasticity. The analysis shows that a reasonably fine uniform mesh of simple 3-noded isoparametric triangular elements was convenient for adequate results. A conservative yet more rational design equation is proposed under the general requirements of the ACI code to compute the nominal shear-friction strength for sand-lightweight CFRC.

References:

[1] The Joint ASCE-ACI Task Committee 426, "The shear strength of reinforced concrete members" Journal of the Structural Division, ASCE, Vol. 99, No. ST6, 1973, pp. 1091-1187.

[2] Kriz, L. B., and Raths, C. H., "Connections in precast concrete structures – strength of corbels" Journal of Prestressed Concrete Institute, Vol. 10, No. 1, 1965, pp. 16-61.

[3] Paulay, T., and Loeber, P. J., "Shear transfer by aggregate interlock" Shear in Reinforced Concrete, ACI Publication SP-42, Vol. 1, 1974, pp. 1-16.

[4] Brikland, P. W., and Birkland H. w., "Connections in precast concrete construction" Journal of the American Concrete Institute, Vol. 63, No. 3, 1966, pp. 345-367.

[5] Mast, R. F., "Auxiliary reinforcement in concrete connections" Journal of the Structural Division, ASCE, Vol. 94, No. ST6, 1968, pp. 1485-1504.

[6] Pastor, M., Mira, P., Rubio, C., and Quencedo, M., "Mesh alignment problems in shear band computations" Proceedings of the US-Europe Workshop on Fracture and Damage in Quasibrittle Structures, Prague, Czech Republic, 21-23 Sept., 1994, pp. 401-408.

[7] ACI Committee 318, "Building code requirements for reinforced concrete, ACI-95 and commentary ACI 318R-95" ACI, 1995, pp. 369.

[8] Mattock, A. H., "Shear transfer in concrete having reinforcement at an angle to the shear plane" Shear in Reinforced Concrete, Publication SP-42, Vol. 1, ACI, 1974, pp. 17-42.

[9] Mattock, A. H., li, W. K., and Wang, T. C., "Shear transfer in lightweight reinforced concrete" Journal of the Prestressed Concrete Institute, Vol. 21, No. 1, 1976, pp. 20-39.

[10] Nichols, G. W., and Ledbetter, W. B., "Bond and tensile capacity of lightweight aggregates" Journal of the American Concrete Institute, Vol. 67, No. 12, 1970, pp. 959-962.

[11] Banthia, N., Mindess, S., and Bentur, A., "Impact behavior of concrete beams" material and Structur RILEM, Vol. 20, No. 119, 1987, pp. 293-302.

[12] Ohama, Y., "Carbon-cement composites" Carbon, Vol. 27, No. 5, 1989, pp. 729-737.

[13] El-Mokadem, K. M., "Shear transfer in concrete reinforced with carbon fibers" Ph.D. Thesis, Oklahoma State University, USA, 2001.

[14] Cervenka, V.: "Constitutive model for cracked reinforced concrete" ACI Journal, Vol. 82, No. 6, 1985, pp. 877-882.

[15] Cervenka, V., Jendele, L., and cervenka, J., "ATENA - program documentation" Part 1 – Theory, Published by Cervenka Consulting, Prague, 2001.

[16] CEB, Comittee Euro-International du Beton, "CEP-FIP Model Code 1990" CEB Bulletin d'information No. 213/214. Thomas Telford, London, 1993.

Notation and symbols

A_c = area of concrete section resisting shear transfer, mm^2

A_{fr} = area of shear friction reinforcement, mm^2

f_c = specified compressive strength of concrete, MPa

f_y = specified yield stress of reinforcement, MPa

P_u = ultimate shear load, N

V_n = nominal shear strength, MPa

ρ = reinforcement ratio, A_{fr} / A_c

μ = coefficient of friction

"سلوك الخرسانة المسلحة بألياف الكربون في القص المباشر بطريقة العناصر المحدودة"

تمثل الخرسانة المسلحة بالألياف الكربونية أحد أشكال التطور المستمر في إنتاج الخرسانة الإنشائية لما تتمتع به من خواص ميكانيكية جيدة وقدرة على التعمير، ولكي يتحقق انتشاراً أوسع لتطبيقات هذا النوع من الخرسانة فإن الأمر يستلزم دراسات وافية لسلوكها تحت تأثير الأحمال والمؤثرات المختلفة. نظراً للطبيعة المعقدة لسلوك الخرسانة تحت تأثير قوى القص، فإن هذا البحث يقدم نموذجاً لدراسة سلوك هذا النوع من الخرسانة تحت تأثير قوى القص المباشر باستخدام طريقة العناصر المحدودة. يشتمل البحث على شرح للأسس النظرية لطريقة الاحتكاك كأحد المفاهيم المعتمدة بالكودين المصري والأمريكي لتحليل القص المباشر باعتباره من أنسب الطرق لتصميم الكوابيل القصيرة، وصلات الخرسانة القديمة والجديدة، وصلات الخرسانة سابقة الصب، وغيرها من التطبيقات العناصر التي يظهر بها مستوى محدد لعمل قوى القص المباشر. يشتمل البحث علي استعراض وشرح لنموذجي مادتي الخرسانة وصلب التسليح وأهم المدخلات المطلوبة.

أوضحت النتائج التحليلية مدي كفاءة النموذج الرياضي المقترح بالمقارنة مع نتائج الاختبارات المعملية المتاحة من الأبحاث السابقة، وإمكانية محاكاة سلوك العينات المختبرة معملياً من حيث التشكلات، الأحمال القصوى، وطبيعة الانهيار باستخدام الخواص الميكانيكية الآتية لتمثيل مادة الخرسانة: مقاومة الضغط، مقاومة الشد، ومعاير المرونة. كما أمكن من خلال النتائج التحليلية استكمال النتائج المطلوبة لاستنباط معادلة تصميميه لتقدير المقاومة القصوى لخرسانة الألياف الكربونية في القص المباشر.